Preparation of two series of VxSiBeta zeolite catalysts with V centres in framework and extra-framework positions and their application in selective oxidation of methanol

Maciej Trejda, Yannick Millot, Karolina Chalupka, Stanislaw Dzwigaj

Preparation of two series of VxSiBeta zeolite catalysts with V centres in framework and extra-framework positions and their application in selective oxidation of methanol

Maciej Trejda[a,*], Yannick Millot[b], Karolina Chalupka[b,c], Stanislaw Dzwigaj[b,*]

[a] Faculty of Chemistry, Adam Mickiewicz University in Poznań, Umultowska 89b, 61-614, Poznan, Poland
[b] Laboratoire de Réactivité de Surface, Sorbonne Université-CNRS, UMR 7197, F-75005, Paris, France
[c] Institute of General and Ecological Chemistry, Technical University of Lodz, Żeromskiego 116, 90 924, Lodz, Poland

Keywords:
Beta
Zeolite
Vanadium
Methanol
Oxidation
Catalysis

A B S T R A C T

Two series of V-containing Beta zeolites have been prepared by contacting of the aqueous NH_4VO_3 solution with two SiBeta zeolites at pH = 2.5 and 6, respectively. Because of the presence in NH_4VO_3 solution at pH = 2.5 mainly monomeric VO_2^+ ions, vanadium have been easily incorporated into framework of SiBeta zeolite as pseudo-tetrahedral non hydroxylated $(SiO)_3V = O$ and hydroxylated $(SiO)_2(OH)V = O$ species. The moderate nucleophilicity of the basic vanadyl oxygen of the latter species play important role in methanol oxidation toward formaldehyde. The selectivity toward formaldehyde on this series of V_xSiBeta(I) increases with the amount of pseudo-tetrahedral hydroxylated $(SiO)_2(HO)V = O$ species, which act as either redox or acidic and basic centres. In contrast at pH = 6, the aqueous NH_4VO_3 solution is expected to contain both mononuclear and polynuclear V ions, thus it is more difficult to incorporate V species in SiBeta at this condition as shown by FT-IR and NMR data. The absence of pseudo-tetrahedral V species in framework position of $V_{0.6}$SiBeta(II) is probably responsible for lack of activity of this catalyst in methanol oxidation. The appearance of this species in the series of V_xSiBeta(II) zeolites for high V content leads to their activity in methanol oxidation toward formaldehyde.

1. Introduction

In the recent decades acidic aluminosilicate zeolites have been used to catalyse many reactions important from the industrial point of view such as cracking, isomerization, alkylation and dehydration because of their high activity and selectivity [1–12]. The catalytic activity of acidic zeolites is related to the proton present with tetrahedral Al(III) atom in the framework of silica with Si(IV) atom to compensate negative charge of aluminosilicate zeolite structure.

Since it is widely accepted that the active sites of redox catalytic processes are tetrahedral transition metal ions [13–28], we have looked for the method that allow removing the Al atoms from the zeolite and then incorporating the transition metal ions in its framework to obtain isolated metal single-site catalyst. However, there is the problem to obtain single-site catalyst with identical and well separated active sites related to two types of complexity, one arising from the oxide support and the other from the precursor aqueous solution.

We have firstly tried to avoid the complexity of the oxide support by selecting zeolite system. In order to have aluminium atoms sufficiently diluted in the zeolite matrix, high silica zeolites such as ZSM-5 or Beta have to be preferred. Apart from its high Si/Al ratio, typically above 10, zeolite Beta, first prepared in 1967 at the Mobil Research and Development Laboratories [29] was selected for the following reasons: i) it has a three-dimensional structure, ii) it possesses pores larger than those of ZSM-5 with 12-membered ring openings (0.75 by 0.57 nm for linear and 0.65 by 0.56 nm for tortuous channels), iii) it exhibits high thermal and acid stability [30].

To avoid the complexity related to the precursor aqueous solution we should pay attention on pH of the aqueous NH_4VO_3 solution and its concentration. As shown from a vanadium species diagram [31] at pH 2.5 vanadium is present in aqueous NH_4VO_3 solution mainly as mononuclear VO_2^+ ions, however at pH 6, vanadium is present mainly as polynuclear V species.

We have shown [32–53] that the incorporation of transition metal ions into the lattice T-atom sites of Beta zeolite was strongly favored when, in the first step, Beta is dealuminated by treatment by nitric acid solution and then, in the second step, the incorporation of transition metal ions resulted from the reaction between the cationic metal

* Corresponding authors.
E-mail addresses: tmaciej@amu.edu.pl (M. Trejda), stanislaw.dzwigaj@upmc.fr (S. Dzwigaj).

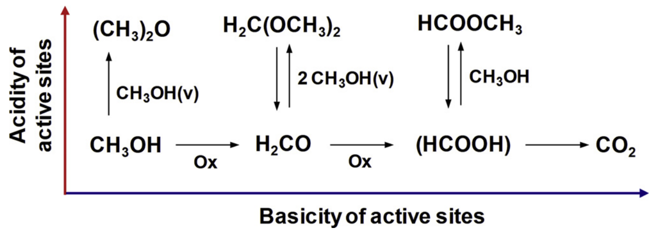

Fig. 1. Scheme of methanol oxidation.

species of the precursor solution at pH 2.5 and the SiO-H groups of vacant T-atom sites created by dealumination of Beta zeolite. So, preparation VSiBeta zeolite at pH = 2.5 allowed incorporating of VO_2^+ ions into zeolite framework and the incorporation at pH 6 was much more difficult and polynuclear V species is incorporated in the extra-framework position.

Methanol oxidation process is widely used in industry in order to obtain formaldehyde as a main product. For this purpose two catalytic systems are applied. In the first one [54], methanol oxidation is performed at relatively high temperature, ca. 823–1023 K, and high methanol concentration, ca. 40%, using catalysts based on silver. In the second method [55], iron-molybdenum metal oxide catalyst is used. The process is performed at lower temperature, ca. 623–723 K, and lower methanol concentration, however more possible side products can be found after reaction. Different products that can be formed make the methanol oxidation process also interesting as a test reaction.

As it was mentioned earlier [56–66], methanol oxidation is a convenient test reaction to identify the active sites of a broad range of catalysts. The possible methanol transformation routs during its oxidation process is presented in Fig. 1. Tatibouët has reported [58], that the reaction network involves two main pathways: i) oxidation by gas phase oxygen or oxide ions from the catalyst (from left to right on Fig. 1) and ii) dehydration which no need of oxygen (from bottom to top on Fig. 1). While dimethyl ether selectivity is generally related to the acidic character of the catalyst employed and to its dehydration ability, the other products require a catalyst with higher basicity or nucleophilic character, suggesting that the acid-base properties of the catalyst can be used to control the catalyst selectivity.

However, the activity and selectivity of catalysts depend on many other factors and in particular the nature and local environment of transition metal species and the most important for vanadium-containing zeolite catalysts are the nature and local environment of vanadium. We have previously shown [32–40,66,67] that environment of vanadium in Beta zeolite can be controlled by using a two-steps post-synthesis method in preparation of VSiBeta zeolite catalyst.

It has been also shown [66] that the catalytic active sites of VSiBeta zeolite are as follows: acidic, highly basic and bifunctional acid-base leading to dimethyl ether, carbon oxides and mild oxidation products, respectively. Because of the strong acidic character of SiBeta in that work, most likely related to the acidic proton of Al-O(H)-Si groups not removed completely upon dealumination step, the high methanol conversion (11.2%) has been observed with 100% selectivity toward dimethyl ether.

In the present work, to realize the deeper dealumination, another sort of tetraethylammonium (TEA) Beta zeolite with higher Si/Al ration of 12.5 has been used. In addition, to remove maximum amounts of Al atoms and associated strong acidic sites (Al-O(H)-Si groups) this TEABeta zeolite was treated by nitric acid (13 mol L^{-1}) at 353 K for 4 h or 5 h. It allowed suppressing strongly the dehydration pathway of methanol conversion on both SiBeta(II) (Si/Al = 1000) and SiBeta(I) (Si/Al = 1300) toward dimethyl ether.

Moreover, in this work, SiBeta(I) (Si/Al = 1300) was used to prepare at pH = 2.5 a series of V_xSiBeta(I) with vanadium in framework as in the case of previous paper [66]. In contrast, SiBeta(II) (Si/Al = 1000) was used to prepare the series of V_xSiBeta(II) at pH = 6 with vanadium present mainly in extra-framework position.

In this paper, we have compared the physicochemical and catalytic properties of two series of V_xSiBeta zeolites with V centres present mainly in framework (V_xSiBeta(I)) and extra-framework (V_xSiBeta(II)) positions. We have shown that the moderate nucleophilicity of the basic vanadyl oxygen of the pseudo-tetrahedral hydroxylated $(SiO)_2(HO)V = O$ species play important role in methanol oxidation toward formaldehyde. The selectivity toward formaldehyde on the series of V_xSiBeta(I) increased with the amount of pseudo-tetrahedral hydroxylated $(SiO)_2(HO)V = O$ species, which acted as either redox or acidic and basic centres. In contrast, the absence of pseudo-tetrahedral hydroxylated $(SiO)_2(HO)V = O$ species in framework position of $V_{0.6}$SiBeta(II) was probably responsible for lack of activity of this catalyst in methanol oxidation. The appearance of this species in the series of V_xSiBeta(II) zeolites for high V content leaded to their activity in methanol oxidation toward formaldehyde.

2. Experimental

2.1. Materials

SiBeta zeolites were prepared by nitric acid (13 mol L^{-1}) treatment of tetraethylammonium Beta zeolite (TEABeta, Si/Al = 12.5) provided by RIPP (China) at 353 K for 5 or 4 h under stirring in air to obtain SiBeta(I) (Si/Al = 1300) and SiBeta(II) (Si/Al = 1000), respectively. The zeolites were contacted with an aqueous NH_4VO_3 solution in excess (2 g of zeolite in 50 ml of solution) at pH = 2.5 or pH = 6, respectively. A concentration of NH_4VO_3 solution varying from 0.25 10^{-2} to 9 10^{-2} mol L^{-1} for both SiBeta zeolites. Because of its low concentration at pH = 2.5, the aqueous NH_4VO_3 solution is expected to contain mainly monomeric VO_2^+ ions [31], in contrast at pH = 6, the aqueous NH_4VO_3 solution is expected to contain mono- and polynuclear V ions [31]. The suspension was left in air for 3 days at room temperature without any stirring. The solids obtained were recovered by centrifugation and dried in air at 353 K overnight. The samples were labeled V_xSiBeta(I) and V_xSiBeta(II) respectively with x = 0.25–4.0 V wt %.

2.2. Techniques

Chemical analysis of the samples was performed with inductively coupled plasma atom emission spectroscopy at the CNRS Center of Chemical Analysis (Vernaison, France).

Powder X-ray diffractograms (XRD) were recorded with a Siemens D5000 apparatus using the CuK_α radiation (λ = 154.05 pm).

Specific surface areas and adsorption isotherms of nitrogen at 77 K were measured with an ASAP 2010 instrument (Micromeritics). All samples were outgassed initially at room temperature then at 623 K until a pressure < 0.2 Pa was reached. The microporous pore volume was determined from the amount of N_2 adsorbed up to P/Po = 0.24.

Infrared spectra were recorded at 298 K in the range 4000 – 400 cm^{-1} with a Bruker Vector 22 FT-IR spectrometer. Samples were pressed at ~ 0.2 ton cm^{-2} into thin wafers of ca. 10 mg cm^{-2} and placed inside the IR cell. Catalysts were outgassed at 673 K for 3 h and then contacted with pyridine (PY) at 423 K for 0.5 h. After saturation with PY, the samples were outgassed at 423, 473, 523 and 573 K for 0.5 h at each temperature. The spectrum of the IR cell alone ("background spectrum") was subtracted from all recorded spectra. The IR spectra of the samples outgassed at 673 K were subtracted from those recorded after adsorption of PY.

FT-IR spectra of zeolites mixed with KBr (1 mg of zeolite was mixed with 200 mg of dehydrated KBr and then 70 mg of this mixture were pressed into a pellet) were registered with a Bruker Vector 22 FT-IR spectrometer (resolution of 4 cm^{-1}).

^{29}Si NMR spectra of samples, transferred at ambient atmosphere into 7 mm zirconia rotors, were recorded with a Bruker Avance spectrometer at 99.4 MHz. The chemical shifts of silicon were measured by reference to tetramethylsilane (TMS). ^{29}Si MAS NMR spectra were obtained at 5 kHz spinning speed, 2.5 μs excitation pulse and 10 s recycle delay.

^{1}H MAS NMR spectra were recorded at 500 MHz with a 90° pulse duration of 3 μs and a recycle delay of 5 s. To record only the proton signal of the sample, the equipment for rotation (12 kHz) was carefully cleaned with ethanol and dried in air at room temperature. The proton signals from probe and rotor were subtracted from the total free induction decay.

^{51}V NMR spectra were recorded with a Bruker Avance 500 spectrometer at 131.6 MHz and with a 2.5-mm zirconia rotor spinning at 30 kHz. The spectra were acquired with spin-echo pulse sequence ($\pi/2-\tau-\pi-\tau$), $\pi/2$ pulse duration of 3.5 μs and 0.5 s recycle delay. Chemical shifts of vanadium were measured by reference to NH_4VO_3 ($\delta = -570$ ppm).

2.3. Methanol oxidation

The methanol oxidation reaction was performed in a fixed-bed flow reactor (Ø 5 mm; length 70 mm). A portion of 0.04 g of catalyst of the size fraction of 0.5 < Ø < 1 mm was placed in the reactor (4 mm height in the reactor). The samples were activated in argon flow (40 mL min^{-1}) at 673 K for 2 h (the rate of heating was 15 K min^{-1}). Then, the temperature was decreased to 523 K. The reactant mixture of Ar/O_2/MeOH (88/8/4 mol%) was supplied at the rate of 40 mL min^{-1}. Methanol (Chempur Poland) was introduced to the flow reactor by bubbling argon gas through a glass saturator filled with methanol. The reactor effluent was analyzed using an online two gas chromatographs. One chromatograph GC 8000 Top equipped with a capillary column of DB-1 operated at 313 K – FID detector was applied for analyses of organic compounds and the second GC containing Porapak Q and 5 A molecular sieves columns for analyses of O_2, CO_2, CO, H_2O and CH_3OH – TCD detector. The columns in the second chromatograph with TCD were heated according to the following program: 5 min at 358 K, increase of the temperature to 408 K (heating rate 5 K min^{-1}), 4 min at 408 K, cooling down to 358 K (for the automatic injection on the column with 5 A), 10 min at 358 K, increase of the temperature to 408 K (heating rate 10 K min^{-1}), 11 min at 408 K. Argon was applied as a carrier gas. The outlet stream line from the reactor to the gas chromatograph was heated at about 373 K to avoid condensation of reaction products. The methanol conversion in the manuscript corresponded to the steady state condition and was expressed as (mmol CH_3OH reacted / mmol CH_3OH in the feed) x 100%.

3. Results and discussion

3.1. Introduction of vanadium in SiBeta zeolites

3.1.1. XRD and BET

The XRD patterns of SiBeta(I) and (II), V_xSiBeta(I) and (II) zeolites are similar and no diffraction reflexes due to other crystalline phases are observed even for $V_{4.0}$SiBeta(I) and (II) samples with high vanadium content. The introduction of vanadium into SiBeta(I) and (II) leads to an increase of the d_{302} spacing as observed in our earlier reports [32,33] indicating an expansion of the Beta structure and suggesting incorporation of vanadium into the framework of both siliceous materials.

Moreover, similar specific surface area for SiBeta(I) and (II), V_xSiBeta(I) and (II) zeolites (655 - 630 m^2 g^{-1}) and absence of extra-framework crystalline compounds for V_xSiBeta(I) and (II) suggest that V ions are well dispersed in both SiBeta zeolites.

3.1.2. FT-IR

The treatment of TEABeta zeolite by aqueous HNO_3 solution leads to the removal of framework Al atoms and the appearance in the FT-IR spectra of SiBeta(I) and (II) (Fig. 2) of a shoulder at 3746 cm^{-1}, an intense band at 3736 cm^{-1} and a broad band at 3520 cm^{-1} respectively due to isolated external, isolated internal and H-bonded silanols [38,68].

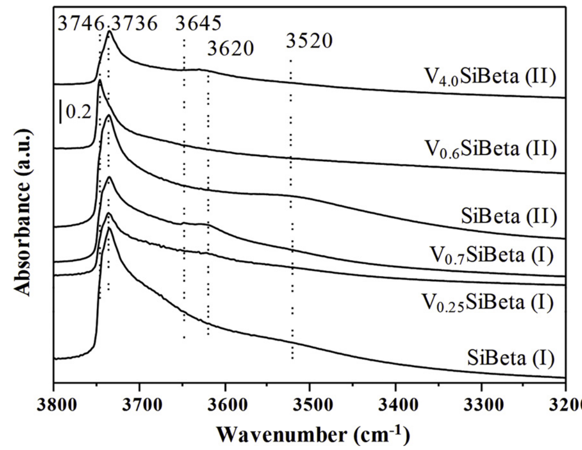

Fig. 2. FTIR spectra recorded at room temperature of SiBeta(I), $V_{0.25}$SiBeta(I), $V_{0.7}$SiBeta(I), SiBeta(II), $V_{0.6}$SiBeta(II) and $V_{4.0}$SiBeta(II) outgassed at 673 K for 3 h (10^{-3} Pa) in the vibrational range of OH groups.

The band at 3520 cm^{-1} reveals the formation of vacant T-atom sites associated with silanol groups in both siliceous zeolites, in line with earlier data for SiBeta zeolite [32,33,66]. The presence of a large amount of silanol groups in SiBeta(I) and (II) is confirmed by the high intensity of a characteristic FT-IR band near 950-960 cm^{-1} (Fig. 3) assigned to the stretching vibration of Si-O vibrators belonging to uncoupled SiO_4 tetrahedra with a hydroxyl groups [32], in line with previous work on silica and various siliceous zeolites [40,69–73].

Upon contact of SiBeta(I) and (II) with the aqueous NH_4VO_3 solution the intensity of the silanol bands at 3736 and 3520 cm^{-1} is

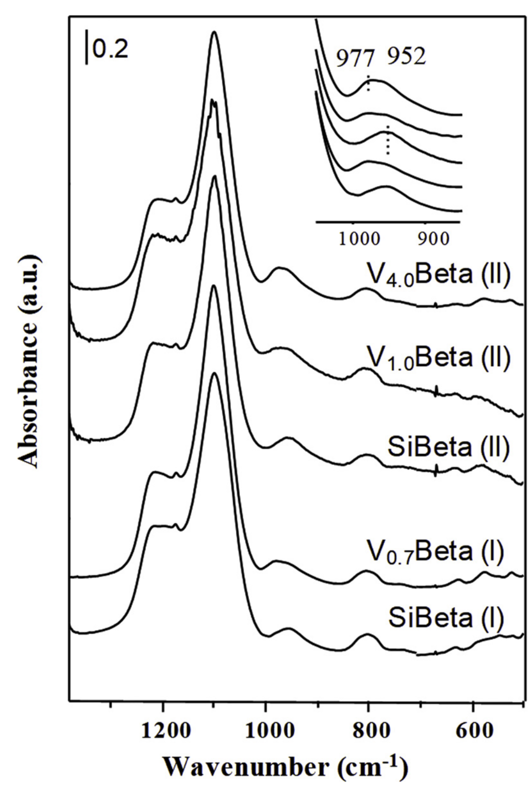

Fig. 3. FTIR spectra (with KBr) recorded at room temperature of SiBeta(I), $V_{0.7}$SiBeta(I), SiBeta(II), $V_{1.0}$SiBeta(II) and $V_{4.0}$SiBeta(II).

reduced, particularly that at 3520 cm^{-1} due to H-bonded SiOH groups (Fig. 2), suggesting that silanol groups interact with the vanadium precursor, in line with earlier report [34,36,74].

However, the interaction of SiBeta with aqueous NH_4VO_3 solution is not the same at pH = 2.5 and 6, as far as the appearance of new IR bands is occurred.

Two FT-IR bands appear at 3645 and 3620 cm^{-1} in SiBeta(I) (pH = 2.5) after incorporation of vanadium ions which are assigned to the hydroxyl vibration of framework $(SiO)_2(HO)V = O$ species located at two different crystallographic sites, in line with earlier data for VSiBeta zeolite [33,36]. The intensity of both bands increases with V content as shown for V_xSiBeta(I) (Fig. 2). Simultaneously, the FT-IR band of the silanol groups at 950-960 cm^{-1} in SiBeta(I) is replaced in $V_{0.7}$SiBEA (I) by two distinct bands at 952 and 977 cm^{-1} (Fig. 3) indicating incorporation of V in Beta zeolite. The bands at 952 and 977 cm^{-1} may be assigned to the Si-O vibrator of silanol groups, polarized via interaction with vicinal V atoms, and the other Si-OV vibrators respectively, as reported earlier [33].

In contrast, upon interaction of SiBeta(II) with the aqueous NH_4VO_3 solution at pH = 6 the bands at 3645 and 3620 cm^{-1} do not appear for low V content (spectrum of $V_{0.6}$ SiBeta(II), Fig. 2) indicating that framework hydroxylated $(SiO)_2(HO)V = O$ species are not formed. This is confirmed by the presence mainly of the FT-IR band of the silanol groups at 950-960 cm^{-1} for $V_{0.6}$SiBeta(II) similar to that of SiBeta(II) (Fig. 3), suggesting that vanadium is not incorporated into the framework within the sensibility of FT-IR spectroscopy. However, the intensity of the bands corresponding to isolated internal and H-bonded SiOH groups strongly decreases (bands at 3736 and 3520 cm^{-1}). In consequence, the isolated external silanols mainly remain on the material surface (band at 3746 cm^{-1}).

For higher amount of V bands appear at 3645 and 3620 cm^{-1} as shown by $V_{4.0}$SiBeta(II) (Fig. 2). However, their low intensity suggests that only part of vanadium is incorporated into the framework of SiBeta (II), as confirmed by the appearance of two distinct bands at 952 and 977 cm^{-1} (Fig. 3).

As reported earlier [32,33,66,74], the pseudo-tetrahedral hydroxylated $(SiO)_2(HO)V = O$ species are in much lower amount in VSiBeta zeolite than their more stable non hydroxylated $(SiO)_3V = O$ analogues (Fig. 4) which have been characterized by DR UV–vis [32,33,66] and DFT calculations [40]. The structure of the $(SiO)_2(HO)V = O$ and $(SiO)_3V = O$ species with the wavenumbers of their associated vibrators has been established on the basis of the above results (SiO-H at 3620 and 3645 cm^{-1}) and earlier data obtained by photoluminescence [74], theoretical calculations [40] and IR and photoacoustic spectroscopies [33].

To determine the acidic centres in SiBeta(I) and (II), V_xSiBeta(I) and (II) we used the FT-IR spectra of adsorbed pyridine taken as probe molecule (Fig. 5).

For SiBeta(I) (Fig. 5), very weak bands typical of pyridinium cations are seen at 1547 and 1638 cm^{-1}, indicating the presence of Brønsted

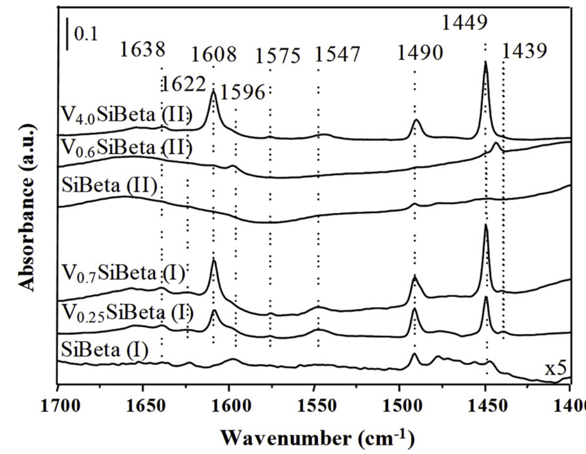

Fig. 5. FTIR spectra recorded at room temperature after adsorption of pyridine at 423 K followed by desorption at 473 K for 0.5 h of SiBeta(I), $V_{0.25}$SiBeta(I), $V_{0.7}$SiBeta(I), SiBeta(II), $V_{0.6}$SiBeta(II) and $V_{4.0}$SiBeta(II).

acidic centres, probably related to the acidic proton of Al-O(H)-Si groups, still present after dealumination. In contrast, for SiBeta(II) those bands are not observed.

Moreover, the bands at 1454 and 1622 cm^{-1} corresponding to pyridine interacting with strong Lewis acidic centres (Al^{3+}) are observed only for SiBeta(I) while those at 1445 and 1596 cm^{-1} (Fig. 5) corresponding to pyridine interacting with weak Lewis acidic centres appear for both SiBeta(I) and SiBeta(II) (Fig. 5).

In V_xSiBeta(I) zeolites, Brønsted acidic centres are generated as shown for $V_{0.25}$SiBeta(I) and $V_{0.7}$SiBeta(I) by the two bands at 1547 and 1638 cm^{-1} appearing after pyridine adsorption (Fig. 5). In contrast, in $V_{0.6}$SiBeta(II) the bands of pyridinium cations at 1547 and 1638 cm^{-1} typical of Brønsted acidic centres are not observed (Fig. 5). The latter only appear for significantly higher V content as shown for $V_{4.0}$SiBeta (II).

For both V_xSiBeta(I) and (II), bands at 1449 and 1608 cm^{-1} appear corresponding to pyridine adsorbed on Lewis acidic centres (V^{5+}). These Lewis acidic centres exhibit a lower strength than that observed in SiBeta(I) and related to Al^{3+} present as traces, as shown by the position of the bands (1608 vs. 1622 cm^{-1}). These bands disappear upon outgassing at increasing temperature (Table 1) as discussed below.

As reported earlier for Beta zeolite [33], the Brønsted acidic centres evidenced in V_xSiBeta(I) and (II) for higher V content are related to the acidic proton of the OH group of framework hydroxylated $(SiO)_2(HO)V = O$ species as deduced from their disappearance upon pyridine adsorption. However, as evidenced earlier for Beta and sodalite systems, only a weak part of all framework tetrahedral V(V) ions appears as such species [40].

The number of acidic centres in V_xSiBeta(I) and (II) zeolites

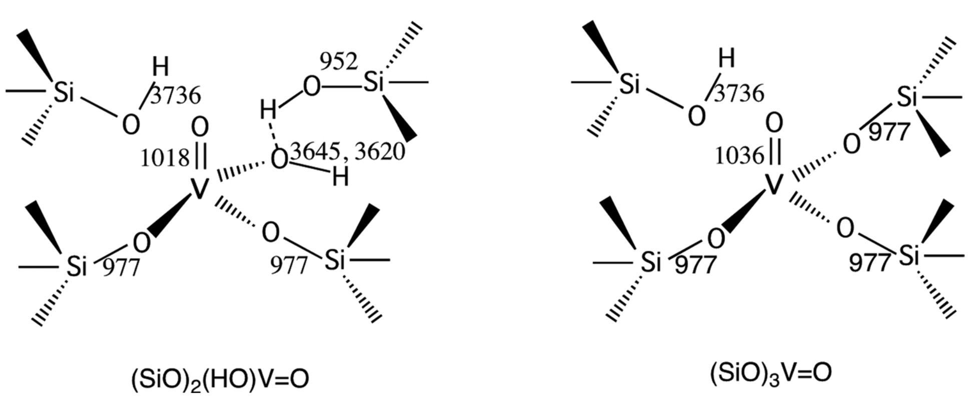

Fig. 4. Schematic representation of the framework pseudo-tetrahedral hydroxylated $(SiO)_2(HO)V = O$ (left) and pseudo-tetrahedral non hydroxylated $(SiO)_3V = O$ (right) species created in V_xSiBeta(I) and V_xSiBeta(II). The wavenumbers 3736, 3645 and 3620, 1018 and 1036, 977 and 952 cm^{-1} correspond to isolated internal SiO-H, VO-H, V = O and Si-O vibrators, respectively.

Table 1
Number of acidic centres of SiBeta and $V_xSiBeta$ zeolites determined from the amount of pyridine remaining adsorbed after outgassing the samples at 473 K (number of Lewis or Brønsted acidic centres), and at 473 and 523 K (total number of acidic centres).

Sample	Lewis acidic centres (x 10^{17})	Brønsted acidic centres (x 10^{17})	total number of acidic centres (x 10^{17})	
			Py desorption at 473 K	Py desorption at 523 K
SiBeta(I)	5.7	8.7	14.4	–
$V_{0.25}$SiBeta(I)	136.7	73.0	209.7	132.7
$V_{0.7}$SiBeta(I)	315.7	57.8	373.5	216.7
$V_{2.0}$SiBeta(I)	36.0	41.4	77.4	45.4
$V_{4.0}$SiBeta(I)	103.8	73.6	177.4	39.8
SiBeta(II)	14.8	–	14.8	–
$V_{0.6}$SiBeta(II)	42.0	–	42.0	17.2
$V_{1.0}$SiBeta(II)	211.5	34.9	246.4	117.7
$V_{4.0}$SiBeta(II)	630.5	82.1	712.6	380.0

calculated from the amount of pyridine outgassed at 473 K for 0.5 h is given in Table 1. The number of Lewis acidic centres increases with the vanadium content for both $V_xSiBeta$(I) an (II) zeolites with a significant decrease for $V_{2.0}$SiBeta(I) and $V_{4.0}$SiBeta(I) suggesting that some vanadium species are present in extra-framework position, possibly as octahedral VO_x oligomers or vanadium oxide clusters where not all vanadium are accessible for pyridine. This is the reason why the number of Brønsted acidic centres is not proportional to the vanadium content in $V_xSiBeta$(I) and (II) zeolites but seems rather to be related to the amount of framework hydroxylated $(SiO)_2(HO)V = O$ species, as shown by Fig. 5 and Table 1.

There are no Brønsted acidic centres in SiBeta(II) and $V_{0.6}$SiBeta(II) samples (Table 1), as evidenced by absence of bands at 3645 and 3620 cm^{-1} (Fig. 2). The Brønsted acidic centres are found in $V_xSiBeta$ (I) and (II) zeolites with high V content (Table 1) when framework hydroxylated $(SiO)_2(HO)V = O$ species appear in both zeolites (Fig. 2, as seen $V_xSiBeta$(II) with bands at 3645 and 3620 cm^{-1}).

Table 1 also gives the total number of acidic centres determined from the amount of pyridine remaining adsorbed after outgassing the samples at 473 and 523 K, making it possible to estimate the acid strength. There is a large difference in the acid strength between the parent SiBeta(I) and (II) zeolites and the resulting V-containing zeolites. For SiBeta(I) and (II), outgassing at 523 K leads to a decrease of 100% of acidic centres compared to the situation after outgassing at 473 K whereas for $V_{0.7}$SiBeta(I) and $V_{1.0}$SiBeta(II) this decrease is *ca.* 42 and 52% respectively. Thus, the acid strength of both $V_xSiBeta$(I) and (II) zeolites appears to increase after incorporation of vanadium in both siliceous SiBeta(I) and (II) zeolites. These results evidence the role of the surroundings of acidic centres on their strength.

3.1.3. 29Si MAS NMR

The ^{29}Si MAS NMR spectra of SiBeta(I) and (II) (Fig. 6) shows four signals at −101.1, -(103.8–103.2), -(111.6–110.9) and -(114.4–113.5) ppm. The latter two signals are due to framework Si atoms in a $Si(OSi)_4$ environment, located at different crystallographic sites, in line with earlier data for Beta [35]. The broad signal at −(101.1–103.8) ppm corresponds to Si atoms in a $Si(OH)(OSi)_3$ environment, as reported earlier for Beta [75], in line with the removal of nearly all Al atoms upon dealumination. The doublet observed at around −101.1 and −(103.8–103.2) ppm for both SiBeta(I) and (II) indicates two types of surroundings of Si atoms in $Si(OH)(OSi)_3$ species.

The attribution of the doublet observed at −101.1 and −(103.8–103.2) ppm to Si atoms in a $Si(OH)(OSi)_3$ environment is confirmed by their increased intensity for the NMR spectrum in CP mode, have already shown in our earlier work [66].

After incorporation of V into SiBeta(I) and (II), the intensity of the

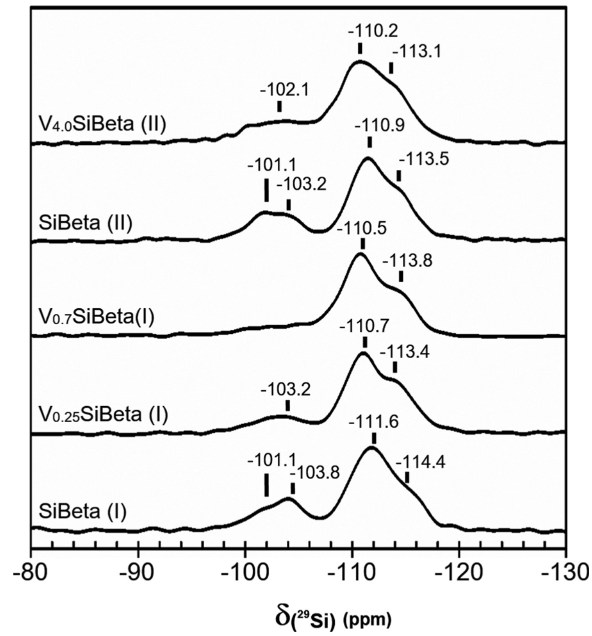

Fig. 6. ^{29}Si MAS NMR spectra recorded at room temperature of SiBeta(I), $V_{0.25}$SiBeta(I), $V_{0.7}$SiBeta(I), SiBeta(II) and $V_{4.0}$SiBeta(II).

signals at -(101.1) and -(103.8 − 103.2) ppm are strongly reduced (Fig. 6), suggesting that the NH_4VO_3 precursor has reacted with SiOH groups of vacant T-atom sites. Moreover, it is important to mention that the incorporation of V into SiBeta(I) is more efficient than that into SiBeta(II) one. As seen from Fig. 6, after incorporation of 0.7 V wt % into SiBeta(I) sample, almost all SiOH groups are consumed, while introduction of 4.0 V wt % into SiBeta(II) sample does not eliminate all SiOH groups.

3.1.4. 1H MAS NMR

The ^{1}H MAS NMR spectra of SiBeta(I) and (II) exhibit two main signals at 4.56 and 1.50 ppm and 5.20 and 1.41 ppm (Fig. 7), respectively. The signals around 1.45 ppm are due to the protons of terminal silanol groups, in line with earlier report [76]. When the zeolite has a low Si/Al ratio, signals at about 3–6 ppm are attributed to Si(OH)Al bridging groups [76,77] and correspond to the Bronsted acidity. Here, a large part of the aluminium atoms was eliminated, so there are few Si (OH)Al bridging groups and just a very weak signal at 3.26 ppm are observed only for SiBeta(II). Then, the main contribution (4.56 and 5.20 ppm) in the corresponding zone of Si(OH)Al bridging groups come from the creation of vacant T-atom sites and thus protons of H-bonded SiOH groups, as shown earlier for different zeolites [78–81].

The disappearance of the signal at 4.56 ppm upon incorporation of V atoms in SiBeta(I) (Fig. 7) evidences the reaction of aqueous NH_4VO_3 solution with protons of H-bonded SiOH groups of vacant T-atom sites. As a result, in $V_{0.25}$SiBeta(I) and $V_{0.7}$SiBeta(I) a new main signal appears at 3.9–3.58 ppm with much lower intensity, likely due to protons of SiOH groups still present in the samples but in strong interaction with incorporated vanadium and associated with an increase in Brønsted acidity (Table 1). It is important to mention here that the SiBeta(I) spectrum was divided by 6.

Moreover, for both $V_{0.25}$SiBeta(I) and $V_{0.7}$SiBeta(I) samples, the signal of the terminal silanol groups is slightly shifted (1.30–1.28 ppm) to that observed for SiBeta(I) support (1.5 ppm), which seems to indicate an interaction with the incorporated vanadium. A very weak-signal at 7.4–7.5 ppm is also present but not yet attributed.

After contact of aqueous NH_4VO_3 solution with SiBeta(II) at pH = 6, much weaker changes are observed with respect to the original ^{1}H MAS NMR spectra, in line with XRD data discussed above. For $V_{1.0}$SiBeta(II)

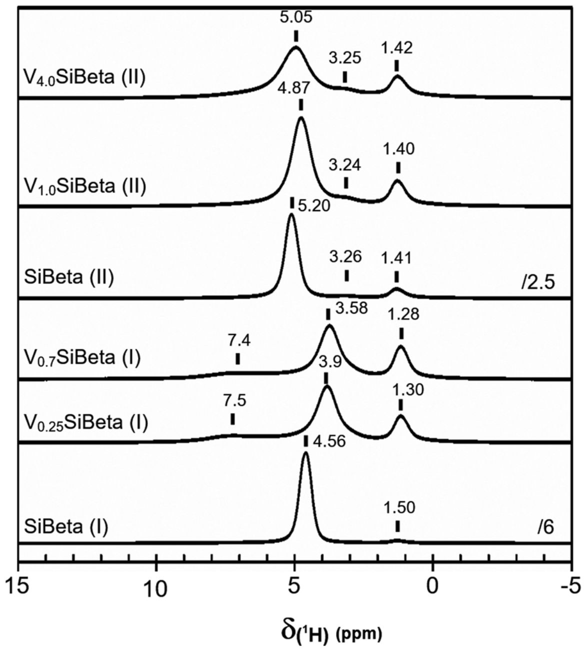

Fig. 7. ^{1}H MAS NMR spectra recorded at room temperature of SiBeta(I), $V_{0.25}$SiBeta(I), $V_{0.7}$SiBeta(I), SiBeta(II), $V_{1.0}$SiBeta(II) and $V_{4.0}$SiBeta(II). To facilitate comparison of the spectra of the samples, the spectra of samples SiBeta (I) and SiBeta(II) were divided by 6 and 2.5, respectively.

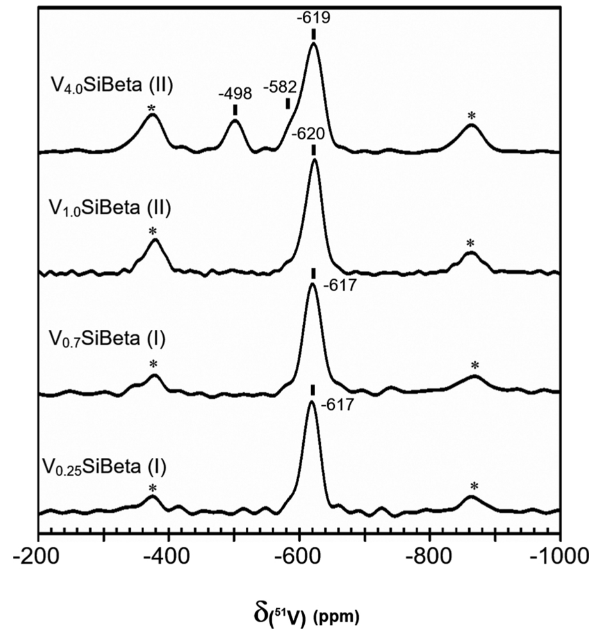

Fig. 8. ^{51}V MAS NMR spectra recorded at room temperature of $V_{0.25}$SiBeta(I), $V_{0.7}$SiBeta(I), $V_{1.0}$SiBeta(II) and $V_{4.0}$SiBeta(II). (*) spinning sidebands.

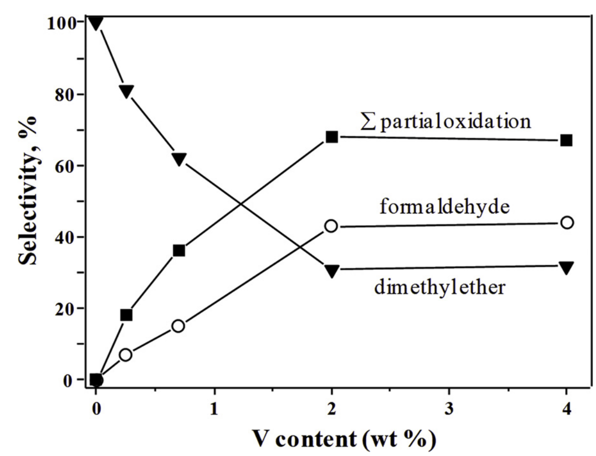

Fig. 9. Product selectivity in methanol oxidation at 523 K plotted as a function of vanadium content. ΣS represents the sum of the selectivities toward partial oxidation products.

and $V_{4.0}$SiBeta(II), the main signal observed at 4.87–5.05 ppm, is slightly reduced and shifted to lower value in comparison to that observed for parent SiBeta(II) zeolite (at 5.20 ppm), suggesting that the protons of H-bonded SiOH groups are little consumed and have a weaker interaction with the vanadium introduced. The much weaker intensity of the signal at 5.05 ppm for $V_{4.0}$SiBeta(II) than that at 5.20 ppm for SiBeta(II) confirms the consumption of part of H-bonded SiOH groups upon contact of the aqueous NH_4VO_3 solution with SiBeta (II) at pH = 6.

Moreover, for both $V_{1.0}$SiBeta(II) and $V_{4.0}$SiBeta(II) samples, the signals at around 1.40–1.42 and 3.24–3.25 ppm are still observed and are very similar to those of SiBeta(II) support (Fig. 6).

The above results clearly suggest that the interaction of aqueous NH_4VO_3 solution with SiBeta(I) and SiBeta(II) at pH = 2.5 and 6 respectively, is not similar and leads to V_xSiBeta(I) and V_xSiBeta(II) with different physicochemical properties as shown by XRD, FT-IR and NMR investigations.

3.2. The coordination of vanadium in V-containing siliceous Beta zeolites

3.2.1. ^{51}V MAS NMR

Pseudo-tetrahedral V species can be characterized by ^{51}V MAS NMR via the signal at around -620 ppm, in line with earlier data for vanadium-containing zeolites [82–84]. Thus, a signal appears at -617 ppm for $V_{0.25}$ SiBeta(I) and $V_{0.7}$SiBeta(I) and at -620 and -619 ppm for $V_{1.0}$SiBeta(II) and $V_{4.0}$SiBeta(II) respectively, are related to the presence of pseudo-tetrahedral V species (Fig. 8).

For $V_{4.0}$SiBeta(II) (Fig. 8), the additional signals at -582 and -498 ppm is probably related to the presence of distorted octahedral V species or VO_x oligomers, in line with earlier work on mesoporous VMCM-41 [84]. For $V_{4.0}$SiBeta(I), in addition to the signal at -617 ppm corresponding to pseudo-tetrahedral V species, the signal at -535 ppm appears (very similar to that observed in our earlier paper [66] (Fig. 9)) with low intensity suggesting the presence in this sample also distorted octahedral V species, probably in extra-framework position.

In conclusion, the above ^{51}V MAS NMR results suggest that for V_xSiBeta(I) zeolites at low V content (x = 0.25 and 0.7 wt %) vanadium is found to be only in pseudo-tetrahedral coordination and at higher content (x = 4.0 wt %) in both pseudo-tetrahedral and octahedral coordinations. In contrast, for V_xSiBeta(II) zeolites with low V content (x = 0.6 wt %) there are no vanadium signals. For higher V content (x = 1.0 wt %) vanadium appears as pseudo-tetrahedral V species and with much higher V content (x = 4 wt %) vanadium is found to be present as framework pseudo-tetrahedral and octahedral V(V) species and also as VO_x oligomers or vanadium oxide, in extra-framework position.

3.3. Oxidation of methanol

As reported earlier [58], acidic and basic centres can be involved in the oxidation of methanol by oxide catalysts. In V_xSiBeta zeolites, non-hydroxylated $(SiO)_3V = O$ and hydroxylated $(SiO)_2(HO)V = O$ species can be considered as either redox or Lewis (V^{5+}) and Brønsted acidic (proton of the OH group) and basic (O^{2-}) centres, on which hydrogen abstraction can take place, as proposed earlier [66].

The first step in the methanol oxidation is suggested to be the

Table 2
Conversion and selectivity determined at 523 K for methanol oxidation on $V_xSiBeta$ zeolites.

Catalysts	Time[a] (min.)	Methanol conversion[b] (%)	Selectivity (%)					
			$(CH_3)_2O$	HCHO	$(CH_3O)_2CH_2$	$HCOOCH_3$	ΣS[c]	CO_2
SiBeta(I)	70	5	100	–	–	–	–	–
$V_{0.25}SiBeta(I)$	70	10	81	7	1	10	18	1
$V_{0.7}SiBeta(I)$	70	5	62	15	2	19	36	2
$V_{2.0}SiBeta(I)$	70	14	31	43	2	23	68	1
$V_{4.0}SiBeta(I)$	70	16	32	44	2	21	67	1
SiBeta(II)	70	2	100	–	–	–	–	–
$V_{0.6}SiBeta(II)$	–	˜ 0	traces	traces	–	–	–	–
$V_{1.0}SiBeta(II)$	70	7	32	49	9	10	68	–
$V_{4.0}SiBeta(II)$	70	5	37	45	9	11	65	–

[a] Time expressed in minutes (min) after which the steady state is reached.
[b] The data correspond to the steady state: (mmol CH_3OH reacted / mmol CH_3OH in the feed) x 100%.
[c] ΣS represents the sum of the selectivities toward partial oxidation products.

abstraction of hydrogen from methanol leading to methoxy species [58]. As reported earlier [85], further transformation of the methoxy species depends on the kind and strength of active centres. In presence of acidic centres only, methoxy group interact with a second CH_3OH molecule to form dimethyl ether, as shown earlier for SiBeta zeolite [66].

In this work, the two SiBeta(I) and (II) zeolites exhibit very small number of acidic centres (Table 1**)**. Methanol oxidation on these samples leads to the formation of dimethyl ether only, with low methanol conversion of 5 and 2% respectively (Table 2).

The IR data on pyridine adsorption (Fig. 4, Table 1) show that both SiBeta(I) and (II) contain only a small amount of Lewis acidic centres. However, Brønsted acidic centres are present only in SiBeta(I), in line with the higher methanol conversion (5 vs 2%). The absence of vanadium species and basic centres in both SiBeta(I) and (II) seems to explain the absence of oxidation products.

The incorporation of a small amount of vanadium in SiBeta(I) leads to a significant increase of methanol conversion with a simultaneous shift of selectivity toward partial oxidation products (Table 2) typical of the redox and acid-base character of $V_xSiBeta$ as reported earlier [66]. The selectivity to dimethyl ether decreases from 100% for SiBeta(I) to 81% for $V_{0.25}SiBeta(I)$ and 62% for $V_{0.7}SiBeta(I)$. Total oxidation to CO_2, which requires the presence of highly basic centres, is not significant on all $V_xSiBeta(I)$ samples.

The increase of V content in $V_xSiBeta(I)$ zeolites leads to an increase of selectivity toward formaldehyde and partial oxidation products (Table 2). As suggested earlier [66], the formaldehyde chemisorbed on acidic centres can desorb as such or be further transformed to formate species.

The presence of basic vanadyl oxygen in the neighborhood of vanadium is required to transform methoxy species into formaldehyde by hydrogen abstraction. This vanadyl oxygen is also involved in the redox cycle of vanadium in the further transformation of chemisorbed formaldehyde into partial oxidation products (e.g. methyl formate). However, the reaction pathway depends on the strength of acidic centres, thus the lower their strength, the easier desorption of formaldehyde. The incorporation of vanadium into SiBeta(I) generates both new Lewis acidic and basic oxygen centres ($V^{5+} = O^{2-}$) as shown by the increase of the number of Lewis acidic centres (Table 1) and the appearance of the FT-IR bands at 3645 and 3620 cm^{-1} assigned to the hydroxyl vibration of framework hydroxylated $(SiO)_2(HO)V = O$ species (Fig. 2).

As proposed earlier [66], the basic vanadyl oxygen of both $(SiO)_3V = O$ and $(SiO)_2(HO)V = O$ species is able to abstract hydrogen from methoxy groups to form formaldehyde but because of the high nucleophilicity of the basic vanadyl oxygen, $(SiO)_3V = O$ species can strongly chemisorb formaldehyde and lead to its full oxidation. However, a very little amount of CO_2 formed in methanol oxidation suggests that $(SiO)_3V = O$ species are not involved in methanol oxidation (Table 2). In contrast, on the less nucleophilic basic vanadyl oxygen of $(SiO)_2(HO)V = O$ species, formaldehyde being less strongly chemisorbed can desorb. As mentioned in our earlier work [66], the proton of framework $(SiO)_2(OH)V = O$ species is likely to be responsible for the Brønsted acidity of $V_xSiBeta$ zeolites. The methoxy species formed on Lewis or Brønsted acidic centres can further react with CH_3OH molecule to form dimethyl ether or can be transformed into formaldehyde in presence of basic centres that abstract hydrogen. For these two reasons, dimethyl ether and formaldehyde are the main products in methanol oxidation on $V_xSiBeta(I)$.

Increasing the vanadium content in $V_xSiBeta(I)$ leads to an increase of conversion and selectivity toward formaldehyde while that toward dimethyl ether decreases (Table 2, Fig. 9). However, only the formaldehyde yield increases with vanadium loading. This suggests that $(SiO)_2(HO)V = O$ species are mainly involved in the transformation of methanol via oxidation path. In contrast, the dimethyl ether yield is almost constant and not related to V content strongly suggesting that dimethyl ether formation does not occur on V sites. In our opinion, the dimethyl ether formation takes place on Bronsted acidic sites and is most likely related to the acidic proton of Al-O(H)-Si groups, present as traces in SiBeta(I) support (Fig. 5) after the dealumination step.

The highest selectivity toward formaldehyde is observed for $V_{4.0}SiBeta(I)$, which exhibits the highest amount of Brønsted acidic centres (Table 1). The decrease of dimethyl ether and the increase of formaldehyde selectivity with increasing vanadium content clearly evidence the role of the less nucleophilic basic vanadyl oxygen of hydroxylated $(SiO)_2(HO)V = O$ species in methanol oxidation toward formaldehyde.

This conclusion is confirmed by the results of methanol oxidation on $V_xSiBeta(II)$. As shown by the data in Table 2, the absence of hydroxylated $(SiO)_2(HO)V = O$ species in $V_{0.6}SiBeta(II)$ is probably responsible for its lack of activity in methanol oxidation. When these pseudo-tetrahedral hydroxylated V species are observed in $V_xSiBeta(II)$, e.g. on $V_{1.0}SiBeta(II)$ and $V_{4.0}SiBeta(II)$ zeolite catalysts (Fig. 2), they are found to be active in the oxidation of methanol (Table 2). However, the presence in $V_{4.0}SiBeta(II)$ of a higher content of VO_x oligomers or vanadium oxide leads to a much lower methanol conversion than in case of $V_{4.0}SiBeta(I)$ with some V content (Table 2).

4. Conclusions

Two series of $V_xSiBeta(I)$ and (II) zeolites were prepared by contacting an aqueous NH_4VO_3 solution in excess with SiBeta(I) (Si/Al = 1300) and SiBeta(II) (Si/Al = 1000) zeolites at pH = 2.5 and 6, respectively.

VO_2^+ ions mostly present in NH_4VO_3 solution at pH = 2.5 were reacted with H-bonded SiOH groups of vacant T-atom sites of SiBeta(I) zeolite. Vanadium was incorporated as pseudo-tetrahedral non hydroxylated $(SiO)_3V = O$ and hydroxylated $(SiO)_2(OH)V = O$ framework species as shown by FT-IR and NMR data. In contrast, at pH = 6, in the presence of mono- and polynuclear V ions in NH_4VO_3 solution, the much lower incorporation of vanadium into framework of SiBeta(II) zeolite was observed.

The number of Brønsted acidic centres found in V_xSiBeta(I) was related to the amount of pseudo-tetrahedral hydroxylated $(SiO)_2$(OH) V = O species. The basic vanadyl oxygen of hydroxylated $(SiO)_2$(HO) V = O species which is less nucleophilic than its non hydroxylated $(SiO)_3$V = O analogue seemed to play an important role in methanol oxidation.

The selectivity toward formaldehyde for the V_xSiBeta(I) series increased with the amount of pseudo-tetrahedral hydroxylated $(SiO)_2$(HO)V = O species, which acted as either redox or acidic and basic centres.

In contrast, preparation of the V_xSiBeta(II) zeolites at pH = 6 did not allow incorporating easily vanadium as pseudo-tetrahedral hydroxylated $(SiO)_2$(OH)V = O framework species as shown by FT-IR and NMR data. The absence of this type of species in $V_{0.6}$SiBeta(II) was probably responsible for the lack of activity of this catalyst in methanol oxidation. The appearance of the pseudo-tetrahedral hydroxylated $(SiO)_2$(OH)V = O species in the V_xSiBeta(II) series for higher V content involve the activity of these catalysts in methanol oxidation.

References

[1] S. Dzwigaj, J. Haber, T. Romotowski, Zeolites 4 (1984) 147.
[2] M. Derewinski, S. Dzwigaj, J. Haber, Zeolites 4 (1984) 214.
[3] W.O. Haag, R.M. Lago, P.B. Weisz, Nature 309 (1984) 589.
[4] B.L. Su, A. Lamy, S. Dzwigaj, M. Briend, D. Barthomeuf, Appl. Catal. 75 (1991) 311.
[5] M.S. Rigutto, H.J.A. de Vries, S.R. Magill, A.J. Hoefnagel, H. van Bekkum, Stud. Surf. Sci. Catal. 78 (1993) 661.
[6] A.I. Biaglow, D.J. Parillo, G.T. Kokotailo, R.J. Gorte, J. Catal. 148 (1994) 213.
[7] G. Bellussi, G. Pazzuconi, C. Perego, G. Girotti, G. Terzoni, J. Catal. 151 (1995) 227.
[8] E.J. Creyghton, S.D. Ganeshie, R.S. Downing, H. van Bekkum, Chem. Commun. (1995) 1859.
[9] K.P. De Jong, C.M.A.M. Mesters, D.G.R. Peferoen, P.T.M. van Brugge, C. de Groot, Chem. Eng. Sci. 51 (1996) 2053.
[10] A.J. Hoefnagel, H. van Bekkum, Micropor. Mesopor. Mater. 35/36 (2000) 345.
[11] C. Perego, P. Ingallina, Catal. Today 73 (2002) 3.
[12] B. Akata, J. Warzywoda, A. Sacco Jr, J. Catal. 222 (2004) 397.
[13] P.B. Venuto, Micropor. Mater. 2 (1994) 297.
[14] A. Corma, Chem. Rev. 97 (1997) 2373.
[15] B. Notari, Adv. Catal. 41 (1996) 253.
[16] A. Corma, M.A. Camblor, P. Esteve, A. Martinez, J. Perez-Pariente, J. Catal. 145 (1994) 151.
[17] A. Thangaraj, S. Sivasanker, P. Ratnasamy, J. Catal. 131 (1991) 394.
[18] B. Kraushaar, J.H.C. van Hooff, Catal. Lett. 2 (1989) 43.
[19] M. Anpo, M. Che, Adv. Catal. 44 (1999) 119.
[20] K. Mori, Y. Miura, S. Shironita, H. Yamashita, Langmuir 25 (2009) 11180.
[21] M. Anpo, T. Kim, M. Matsuoka, Catal. Today 470 (2009) 269.
[22] M. Anpo, S. Dzwigaj, M. Che, Adv. Catal. 52 (2009) 1.
[23] Y. Hu, Y. Nagai, D. Rahmawaty, C. Wei, M. Anpo, Catal. Lett. 124 (2008) 80.
[24] M. Matsuoka, T. Kamegawa, M. Anpo, Stud. Surf. Scie. Catal. 165 (2007) 725.
[25] H. Yamashita, S. Kawasaki, S. Yuan, K. Maekawa, M. Anpo, M. Matsumura, Catal. Today 126 (2007) 375.
[26] T. Kamegawa, J. Morishima, M. Matsuoka, J.M. Thomas, M. Anpo, J. Phys. Chem. C 111 (2007) 1076.
[27] T. Kamegawa, T. Shudo, H. Yamashita, Top. Catal. 53 (2010) 555.
[28] H. Yamashita, S. Kawasaki, Y. Ichihashi, M. Harada, M. Takeuchi, M. Anpo, G. Stewart, M.A. Fox, C. Louis, M. Che, J. Phys. Chem. B 102 (1998) 5870.
[29] R.L. Wadlinger, G.T. Kerr, E.J. Rosinski, US Patent 3308069 (1967).
[30] J.B. Higgins, R.B. LaPierre, J.L. Schlenker, A.C. Rohrman, J.D. Wood, G.T. Kerr, W.J. Rohrbaugh, Zeolites 8 (1988) 446.
[31] C.F. Baes Jr, R.E. Mesmer, The Hydrolysis of Cations, Krieger Publishing Company, Malabar, 1986, p. 210 Reprint Edition.
[32] S. Dzwigaj, M.J. Peltre, P. Massiani, A. Davidson, M. Che, T. Sen, S. Sivasanker, J. Chem. Soc. Chem. Commun. (1998) 87.
[33] S. Dzwigaj, P. Massiani, A. Davidson, M. Che, J. Mol. Catal. 155 (2000) 169.
[34] S. Dzwigaj, M. Matsuoka, M. Anpo, M. Che, J. Phys. Chem. B 104 (2000) 6012.
[35] S. Dzwigaj, E.M. El Malki, M.J. Peltre, P. Massiani, A. Davidson, M. Che, Top. Catal. 11/12 (2000) 379.
[36] R. Hajjar, Y. Millot, P.P. Man, M. Che, S. Dzwigaj, J. Phys. Chem. C 112 (2008) 20167.
[37] S. Dzwigaj, Cur. Opin. Solid State Mater. Scie. 7 (2003) 461.
[38] S. Dzwigaj, E. Ivanova, R. Kefirov, K. Hadjiivanov, F. Averseng, J.M. Krafft, M. Che, Catal. Today 142 (2009) 185.
[39] P. Pietrzyk, Z. Sojka, S. Dzwigaj, M. Che, J. Am. Chem. Soc. 129 (2007) 14174.
[40] F. Tielens, M. Catayud, S. Dzwigaj, M. Che, Micropor. Mesopor. Mater. 119 (2009) 137.
[41] S. Dzwigaj, M. Che, J. Phys. Chem. B 110 (2006) 12490.
[42] J. Janas, T. Machej, J. Gurgul, R.P. Socha, M. Che, S. Dzwigaj, Appl. Catal. B 75 (2007) 239.
[43] J. Janas, T. Shishido, M. Che, S. Dzwigaj, Appl. Catal. B 89 (2009) 196.
[44] S. Dzwigaj, J. Janas, T. Machej, M. Che, Catal. Today 119 (2007) 133.
[45] S. Dzwigaj, L. Stievano, F.E. Wagner, M. Che, J. Phys. Chem. Solids 68 (2007) 1885.
[46] J. Janas, J. Gurgul, R.P. Socha, T. Shishido, M. Che, S. Dzwigaj, Appl. Catal. B 91 (2009) 113.
[47] K. Hadjiivanov, E. Ivanova, R. Kefirov, J. Janusz, A. Plesniar, S. Dzwigaj, M. Che, Micropor. Mesopor. Mater. 131 (2010) 1.
[48] S. Dzwigaj, J. Janas, J. Mizera, J. Gurgul, R.P. Socha, M. Che, Catal. Lett 126 (2008) 36.
[49] J. Janusz, J. Gurgul, R.P. Socha, S. Dzwigaj, Appl. Catal. B 91 (2009) 217.
[50] S. Dzwigaj, J. Janas, J. Gurgul, R.P. Socha, T. Shishido, M. Che, Appl. Catal. B 85 (2009) 131.
[51] S. Dzwigaj, T. Shishido, J. Phys. Chem. C 112 (2008) 5803.
[52] K. Hadjiivanov, A. Penkova, R. Kefirov, S. Dzwigaj, M. Che, Micropor. Mesopor. Mater. 124 (2009) 59.
[53] J. Janas, J. Gurgul, R.P. Socha, J. Kowalska, K. Nowinska, T. Shishido, M. Che, S. Dzwigaj, J. Phys. Chem. C 113 (2009) 13273.
[54] C.H. Bartholomew, R.J. Farrauto, Fundamentals of Industrial Catalytic Processes, John Wiley & Sons, Inc., 2005.
[55] A.P. Vieira Soares, M. Farinha Portela, A. Kinnemann, Chem. Rev. 47 (2005) 125.
[56] C. Louis, J.M. Tatibouët, M. Che, J. Catal. 109 (1988) 354.
[57] J.M. Tatibouët, M. Che, M. Amirouche, M. Fournier, C. Rocchiccioli-Deltcheff, J. Chem. Soc., Chem. Commun. (1988) 1260.
[58] J.M. Tatibouët, Appl. Catal. A 148 (1997) 213.
[59] R.Z. Khaliullin, A.T. Bell, J. Phys. Chem. B 106 (2002) 7832.
[60] M. Trejda, J. Kujawa, M. Ziolek, Catal. Lett. 108 (2006) 141.
[61] I. Sobczak, N. Kieronczyk, M. Trejda, M. Ziolek, Catal. Today 139 (2008) 188.
[62] K. Bruckman, J.M. Tatibouët, E. Serwicka, J. Haber, J. Catal. 139 (1993) 455.
[63] M. Che, C. Louis, J.M. Tatibouët, Polyhedron 5 (1986) 123.
[64] L.J. Burcham, I.E. Wachs, Catal. Today 49 (1999) 467.
[65] X. Gao, I.E. Wachs, M.S. Wong, J.Y. Ying, J. Catal. 203 (2001) 18.
[66] M. Trejda, M. Ziolek, Y. Millot, K. Chalupka, M. Che, S. Dzwigaj, J. Catal. 281 (2011) 169.
[67] D.C. Tranca, F.J. Keil, I. Tranca, M. Calatayud, S. Dzwigaj, M. Trejda, F. Tielens, J. Phys. Chem. C 281 (2015) 169.
[68] M. Trombetta, G. Busca, L. Storaro, M. Lenarda, M. Casagrande, A. Zambon, Phys. Chem. Chem. Phys. 2 (2000) 3529.
[69] M. Decottignies, J. Phalippou, J. Zarzycki, J. Mater. Sci. 13 (1978) 2605.
[70] R. Soda, Bull. Chem. Soc. Jpn 34 (1961) 1491.
[71] A. Duran, C. Serna, V. Fornes, J.M. Fernandez-Navarro, J. Non-Cryst. Solids 82 (1986) 69.
[72] M. Hino, T. Sato, Bull. Chem. Soc. Jpn 44 (1971) 33.
[73] M. Ocana, V. Fornes, C.J. Serna, J. Non-Cryst. Solids 107 (1989) 187.
[74] S. Dzwigaj, M. Matsuoka, R. Franck, M. Anpo, M. Che, J. Phys. Chem. B 102 (1998) 6309.
[75] E. Bourgeat-Lami, F. Fajula, D. Anglerot, T. des Courières, Micropor. Mater. 1 (1993) 237.
[76] Yijiao Jiang, Jun Huang, Weili Dai, Michael Hunger, Solid state NMR 39 (2011) 116–141.
[77] MaríaDolores González, Yolanda Cesteros, Pilar Salagre, Microporous Mesoporous Mater. 144 (2011) 162–170.
[78] C. Pazé, A. Zecchina, S. Spera, A. Cosma, E. Merlo, G. Spano, G. Girotti, Phys. Chem. Chem. Phys. 1 (1999) 2627.
[79] L.W. Beck, J.F. Haw, J. Phys. Chem. 99 (1995) 1076.
[80] A. Zecchina, S. Bordiga, G. Spoto, L. Marchese, G. Petrini, G. Leofanti, M. Padovan, J. Phys. Chem. 96 (1992) 4991.
[81] G.I. Woolery, L.B. Alemany, R.M. Dessau, A.W. Chester, Zeolites 6 (1986) 14.
[82] G. Centi, S. Perathoner, F. Trifiro, A. Aboukais, C.F. Aïssi, M. Guelton, J. Phys. Chem. 96 (1992) 2617.
[83] B.I. Whittington, J.R. Anderson, J. Phys. Chem. 97 (1993) 1032.
[84] B. Sulikowski, Z. Olejniczak, E. Wloch, J. Rakoczy, R.X. Valenzuela, V. Cortés Corberan, Appl. Catal. A 232 (2002) 189.
[85] G. Busca, A.S. Elmi, P. Forzatti, J. Phys. Chem. 91 (1987) 5263.